TISSUE ENGINEERING: Part A
Volume 17, Numbers 9 and 10, 2011

DOI: 10.1089/ten.tea.2010.0481

Hyaluronic Acid Hydrogels Support Cord-Like Structures from Endothelial Colony-Forming Cells

Derek Yee, B.S.,[1–3,*] Donny Hanjaya-Putra, B.S.,[1,2,*] Vivek Bose,[1,2]
Eli Luong, B.S.,[1,3] and Sharon Gerecht, Ph.D.[1,2]

The generation of functional vascular networks has the potential to improve treatment for vascular diseases and to facilitate successful organ transplantation. Endothelial colony-forming cells (ECFCs) have robust proliferative potential and can form vascular networks *in vivo*. ECFCs are recruited from a bone marrow niche to the site of vascularization, where cues from the extracellular matrix instigate vascular morphogenesis. Although this process has been elucidated using natural matrix, little is known about vascular morphogenesis by ECFCs in synthetic matrix, a xeno-free scaffold that can provide a more controllable and clinically relevant alternative for regenerative medicine. We sought to study hyaluronic acid (HA) hydrogels as three-dimensional scaffolds for capillary-like structure formation from ECFCs, and to determine the crucial parameters needed to design such synthetic scaffolds. We found that ECFCs express HA-specific receptors and that vascular endothelial growth factor stimulates hyaluronidase expression in ECFCs. Using a well-defined and controllable three-dimensional HA culture system, we were able to decouple the effect of matrix viscoelasticity from changes in adhesion peptide density. We determined that decreasing matrix viscoelasticity, which corresponds to a loose ultrastructure, significantly increases ECFC vascular tube length and area, and that the effect of local delivery of vascular endothelial growth factor within the hydrogel depends on the makeup of the synthetic environment. Collectively, these results set forth initial design criteria that need to be considered in developing vascularized tissue constructs.

Introduction

Generating a functional vascular network within a three-dimensional (3D) synthetic scaffold has the potential to improve treatment for vascular disease and to facilitate successful organ transplantation. Since their discovery, marrow-derived circulating endothelial progenitor cells (EPCs) have been considered to participate in postnatal vasculogenesis.[1–3] Putative EPCs have been proposed as a potential therapeutic tool for treating vascular disease—either to be infused into the site of vascularization[4,5] or to be expanded *ex vivo* to engineer vascularized tissue constructs.[6–8] It has become more evident that endothelial colony-forming cells (ECFCs), a subtype of EPC recently identified from circulating adult and human umbilical cord blood, express characteristics of putative EPCs.[9] These ECFCs are characterized by a robust proliferative potential to form secondary and tertiary colonies, as well as by *de novo* blood vessel formation *in vivo*.[10,11]

In response to vascular endothelial growth factor (VEGF), ECFCs are mobilized from their bone marrow niche, circulated along the endothelium, and recruited to the site of vascularization.[12] Administration of VEGF at the site of ischemia has been reported to restore blood flow.[13] To further participate in neovascularization, ECFCs need to degrade the basement membrane, interact with neighboring cells, and initiate vascular morphogenesis.[3] Evidently, the extracellular matrix (ECM) provides biophysical and biochemical signals for ECFCs to form stable and functional blood vessels. Adult ECM is composed of various components, including hyaluronic acid (HA), a nonsulfated glycosaminoglycan. HA is most abundant during early embryogenesis; it then becomes ubiquitously distributed at the onset of differentiation,[14] where it plays a critical role in regulating the angiogenic process. HA facilitates cells adhesion, proliferation, migration, and morphogenesis through its two surface receptors, CD44 and CD168.[15]

In the last decades, our understanding of the role of the ECM in vascular morphogenesis has been widely expanded, due to well-defined *in vitro* angiogenesis models. Although the molecular mechanisms that regulate endothelial cells to form capillary-like structures (CLSs) in collagen and fibrin

[1]Department of Chemical and Biomolecular Engineering, The Johns Hopkins University, Baltimore, Maryland.
[2]Johns Hopkins Physical Sciences-Oncology Center and Institute for NanoBioTechnology, The Johns Hopkins University, Baltimore, Maryland.
[3]Department of Biomedical Engineering, The Johns Hopkins University, Baltimore, Maryland.
*These two authors contributed equally to this work.

gels has been elucidated in great detail,[16,17] very few studies have investigated vascular morphogenesis in a synthetic matrix, a xeno-free scaffold that is more clinically relevant for regenerative medicine.[18,19] HA hydrogels can be made of well-defined synthetic polymer networks that have not only a high water content to promote cells viability, but also biophysical and biochemical properties similar to many soft tissues,[20,21] and these properties can be tuned to favor vascular morphogenesis. We have previously reported that HA hydrogels can support two-dimensional (2D) tubulogenesis of ECFCs.[22] Here, we extended our previous study to explore 3D vascular morphogenesis of ECFCs for the initial step in creating vascularized engineered constructs for therapeutic tissue vascularization. We first demonstrate that ECFCs express the HA receptors CD44 and CD168 and that high levels of VEGF upregulate the expression of hyaluronidase in ECFCs. We then examine HA hydrogels for CLS formation from ECFC and show that vascular morphogenesis only occurs in softer matrices, which correspond to a loose ultrastructure, and that the local delivery of VEGF within the HA hydrogels only slightly enhances ECFC tube formation in the softer matrix compared to VEGF supplementation in the culture media. These findings establish some of the crucial parameters needed to induce vascularization in synthetic HA hydrogels.

Materials and Methods

Human ECFCs

Human umbilical cord blood ECFCs were isolated from outgrowth clones (kindly provided by Dr. Yoder, Indiana University School of Medicine), expanded in endothelial growth media (EGM; PromoCell GmbH), and used for experiments between passages 6 and 8, as we previously described.[22,23]

Preparation of HA hydrogels

Heprasil hydrogels (Glycosan BioSystem, Inc.) were prepared by mixing 1% w/v CMHA-S (99.7 wt%) and HP-DTPH (0.3 wt%) solution (Heprasil) with 1% w/v Gtn-DTPH solution (Gelin-S) in a 1:1 volume ratio with 0.22%, 0.11%, and 0.059% (w/v) of polyethylene (glycol) diacrylate (PEGDA) crosslinker (MW 3400) in a 4:1 volume ratio. The hydrogels were cast into a 96-well glass bottom plate (MatTek) and allowed to gel at 37°C for 1 h before EGM medium was added.

Viscoelasticity measurement

We obtained oscillatory shear measurements of the elastic modulus (G') using a constant strain rheometer with steel cone-plate geometry (25 mm in diameter; RFS3; TA Instruments), as previously described.[21,22] Briefly, oscillatory time sweeps were performed on three samples ($n=3$) for 0.22%, 0.11%, and 0.059% (w/v) hydrogels to monitor the *in situ* gelation. The strain was maintained at 20% during the time sweeps by adjusting the stress amplitude at a frequency of 1 Hz. This strain and frequency were chosen because G' was roughly frequency-independent within the linear viscoelastic regime. The 24-h tests occurred in a humidified chamber at a constant temperature (25°C) at 30-s intervals. The Young's modulus (substrate viscoelasticity) was calculated by $E=2G'(1+v)$. HA-gelatin hydrogels can be assumed to be incompressible,[21] such that their Poisson's ratios (v) approach 0.5 and the relationship becomes $E=3G'$.[24,25]

Scanning electron microscopy

The ultrastructure of the hydrogels was studied using scanning electron microscopy (SEM) (FEI Quanta ESEM 200), as previously described.[26] Briefly, the hydrogels were swelled in phosphate-buffered saline (PBS) for 24 h, quickly frozen in liquid nitrogen, and then freeze-dried in a Virtis Freeze Dryer under vacuum at −50°C for 3 days, until the samples became completely dry. The freeze-dried hydrogels were fractured carefully to reveal their interiors, mounted onto aluminum stubs with double-sided carbon tape, and sputter-coated (Anatech Hummer 6.2 Sputter Coater) with Ag for 1 min. We examined the interior morphology of the hydrogels using SEM at 25 kV and 12 nA.

Angiogenesis assay

Human umbilical cord blood ECFCs were encapsulated in 0.22% w/v, 0.11% w/v, and 0.059% w/v HA hydrogels with densities of 2.10^6 cells/mL. To ensure 3D setting, constructs were prepared and placed on top of a thin film of 30 μL substrate-only created from the corresponding w/v percent. To study the local delivery of VEGF, 50 ng/mL of VEGF is encapsulated together with the cells suspension to form the 3D constructs. In all cases, constructs were cultured for up to 48 h in EGM (PromoCell GmbH) supplemented with 1 or 50 ng/mL recombinant human $VEGF_{165}$ (Pierce). Observation and image acquisition were performed using an inverted light microscope (Olympus IX50) and a confocal microscope (LSM 510 Meta; Carl Zeiss Inc.) at time intervals of 24 and 48 h.

VEGF released profile study

At various time points, 1 mL of the conditioned medium from each gel type was collected and replaced with a fresh growth medium. At a final time point (48 h), the gels were degraded using endogenous 1000 IU/mL hyaluronidase IV (Sigma) for 24 h and the media were collected. All the samples ($n=3$) were stored at −80°C before analysis. VEGF release profile was performed using an ELISA kit (Pierce Biotechnology) following manufacturer's instructions and as was reported in our previous publications.[27,28] Briefly, $VEGF_{165}$ in the ELISA kit standards and samples were captured on the anti-human $VEGF_{165}$ antibody-coated microplate. After removing unbound proteins, biotinylated antibody reagent was added to bind to the secondary site on $VEGF_{165}$. Then, to produce a colorimetric signal, streptavidin-horseradish peroxidase was added to bind to tetramethyl benzidine (TMB). Standards were prepared according to the manufacturer's instructions. Plate washing was performed three times between each step to remove any excess reagents. The colorimetric signal was detected using a UV microplate spectrophotometer (SpectraMax Plus; Molecular Devices) at absorbance wavelengths of 450 and 550 nm. The standard curve was interpolated to determine the amount of VEGF165 at each predetermined time point. Results are presented in terms of cumulative release as a function of time.

Fluorescence-activated cell sorting/Flow cytometry

Human umbilical cord blood ECFCs were treated with 0.05% trypsin for 5 min, counted, separated into $\sim 1\times10^6$

cells per vial, and fixed with 3.7% formaldehyde for 10 min. Cells were then incubated in mouse anti-human CD44 (1:200; Sigma) for 1 h. Cells were rinsed with PBS, and then incubated in anti-mouse IgG FITC conjugate (1:50; Molecular Probes) for 1 h. Afterward, cells were strained and suspended in 0.1% bovine serum albumin. All analysis was done using isotype controls corresponding to each specific antibody. User guide instructions were followed to complete the fluorescence-activated cell sorting analysis.

Immunofluorescence

Human umbilical cord blood ECFCs cultured in flasks or encapsulated ECFCs cultured within HA hydrogels for 48 h were fixed using formalin-free fixative (Accustain; Sigma) for 20 min and washed with PBS. For staining, cells were permeabilized with a solution of 0.1% Triton-X for 10 min; washed with PBS; incubated for 1 h with anti-human CD44 (1:100; Sigma), or anti-human CD168 (1:50; Novocastra); rinsed twice with PBS; and incubated with anti-mouse IgG Cy3 (1:50; Sigma) After rinsing twice with PBS, cells were incubated with either FITC-conjugated lectin (1:40; Vector) or FITC-conjugated phalloidin (1:40; Molecular Probes) for 1 h, rinsed with PBS, and incubated with 4′6-diamidino-2-phenylindole (DAPI) (1:1000; Roche Diagnostics) for an additional 10 min. The hydrogels were directly imaged by inverted fluorescence microscopy in the 96-well glass bottom plate. The immunolabeled cells were examined using confocal microscopy (LSM 510 Meta; Carl Zeiss Inc.).

Quantification of CLSs

The LIVE/DEAD Viability/Cytotoxicity Kit (Invitrogen) was used to observe CLSs, following the manufacturer's protocol. Briefly, calcein AM dye was diluted in phenol red-free Dulbecco's modified Eagle's medium (Invitrogen) to obtain a final concentration of 2 μM. The constructs were incubated with the dye solution for 30 min. After replacing with fresh phenol red-free Dulbecco's modified Eagle's medium, CLSs were observed using a fluorescent microscope with a 10× objective lens (Axiovert; Carl Zeiss, Inc.). We analyzed four image fields per construct from three distinct experiments ($n = 3$) performed in triplicate, using Metamorph software 6.1 (Universal Imaging Corp.) to quantify and compare CLSs formed within each hydrogel.

Real-time reverse transcriptase-polymerase chain reaction

Two-step reverse transcriptase (RT)-polymerase chain reaction (PCR) was performed on ECFCs cultured in media supplemented with 1 or 50 ng/mL VEGF. The human breast cancer cell line MDA-MB-231 and colon carcinoma cell line LS174T (both from ATCC) were used as a positive control. Total RNA was extracted using TRIzol (Gibco, Invitrogen) according to the manufacturer's instructions. Total RNA was quantified by an ultraviolet spectrophotometer, and the samples were validated for no DNA contamination. RNA (1 μg per sample) was reversed transcribed using M-MLV (Promega Corp.) and oligo(dT) primers (Promega Corp.) according to the manufacturer's instructions. We used the TaqMan Universal PCR Master Mix and Gene Expression Assay (Applied Biosystems) for *SPAM1*, *HPRT1*, and *β-ACTIN*, according to the manufacturer's instructions. The TaqMan PCR step was performed in triplicate with a StepOne Real-Time PCR system (Applied Biosystems), using the manufacturer's instructions. The relative expression of *SPAM1* was normalized to the amount of *HPRT1 or β-ACTIN* in the same cDNA by using the standard curve method described by the manufacturer. For each primer set, the comparative computed tomography method (Applied Biosystems) was used to calculate amplification differences among the different samples. The values for experiments ($n = 3$) were averaged and graphed with standard deviations.

Statistical analysis

Analysis of CLS quantification and hyaluronidase expression data was performed on triplicate samples with quadruplicate and duplicate readings at each data point, respectively, and statistical analysis was performed using GraphPad Prism 4.02 (GraphPad Software, Inc.). T-tests were performed to determine significance using GraphPad Prism 4.02 (GraphPad Software Inc.). Significance levels, determined using posttests among the three substrates, were set at $^{*}p < 0.05$, $^{**}p < 0.01$, and $^{***}p < 0.001$, respectively. All graphical data were reported.

Results

CD44, CD168, and hyaluronidase expression by ECFCs

We first investigated whether ECFCs could interact with HA-based hydrogels. HA is known to participate in the formation, alignment, and migration of the capillary plexus in early embryonic development.[29] Further, during development, cellular interactions with HA are mediated by CD44 and CD168. CD44 is involved in the initial binding of HA to the cell surface before its internalization and degradation by acid hydrolases. CD168 is involved in HA-induced cell locomotion.[30] We therefore investigated whether ECFCs could interact with HA-based hydrogels. During *in vitro* culture, human umbilical cord blood ECFCs were found to express high levels of CD44 (Fig. 1A). In fact, ECFCs could be easily observed by staining for CD44 (Fig. 1Bi), whereas the expression of CD168 was more difficult to detect (Fig. 1Bii). ECFCs were characterized by membrane expression of CD44 (Fig. 1Ci) and intracellular expression of CD168 (Fig. 1Cii). To examine the potential of ECFCs to remodel the HA hydrogel, real-time reverse transcriptase (RT)-PCR was performed to examine hyaluronidase expression. We found that high concentrations of VEGF upregulated its expression in ECFCs to levels comparable to colon cancer cells, which are known to produce hyaluronidase during tumor growth and invasion (Fig. 1D).[31]

HA hydrogels for 3D in vitro *tubulogenesis*

In this study, we used HA-based hydrogels to study 3D tube morphogenesis by ECFCs. HA hydrogels have the advantage that the chemistry of the network is easily controlled via reaction conditions and is uniform among the various batches, which is difficult or impossible to achieve with naturally derived matrices, such as Matrigel and collagen. Further, while the enzymatic crosslinking of such natural gels as Matrigel and collagen allows studies of increased viscoelasticity, chemically modified HA-based hydrogels enable control over crosslink density, thus offering an opportunity to

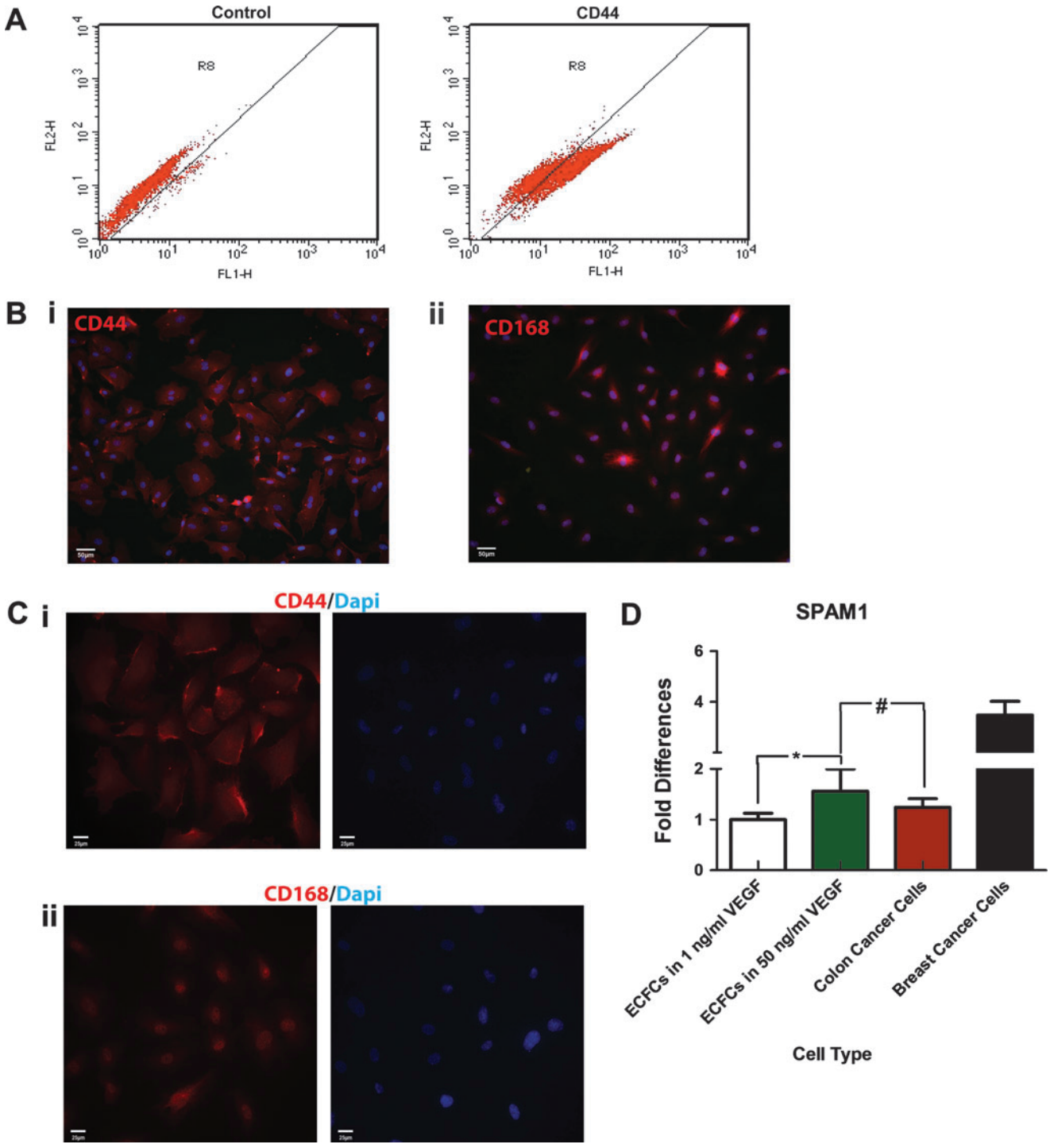

FIG. 1. CD44 and CD168 expression and Hyal production by ECFCs. **(A)** Flow cytometry analysis revealed that human umbilical cord blood ECFCs express CD44. **(B)** Using immunofluorescence staining, **(i)** ECFCs were observed using CD44 (red; nuclei in blue), whereas **(ii)** the expression of CD168 was more difficult to detect (red; nuclei in blue). **(C)** Higher magnification revealed **(i)** membrane expression of CD44, and **(ii)** intracellular expression of CD168 (both in red; nuclei in blue). **(D)** Expression of hyaluronidase in ECFCs increase in high VEGF media, with levels comparable to colon cancer cells. Significance levels were set at: $^{\#}p > 0.05$ and $^{*}p < 0.05$. Scale bar is 100 μm. ECFC, endothelial colony-forming cell; VEGF, vascular endothelial growth factor.

study cellular responses to a wide range of tunable physical stimuli alone, without the effect of changes in adhesion peptide density. Previous studies demonstrated that HA-based hydrogels support *in vitro* 2D tubulogenesis[22] and *in vivo* angiogenesis,[32] as well as embryonic vasculogenesis.[33] For the present study, we utilized thiol-modified HA-gelatin hydrogels to encourage ECFC attachment. These hydrogels can be mechanically tuned using the PEGDA crosslinker while pre-

serving the uniform presentation of cell adhesion molecules,[21] which is difficult to obtain using naturally derived matrices. We generated different hydrogels with the same HA:gelatin ratio, but with increased PEGDA crosslinker concentrations, and examined the gelation kinetics. We show that, within 12 h of curing, a distinct Young's modulus (viscoelasticity) profile is established for 0.22% w/v (640 Pa), 0.11% w/v (73 Pa), and 0.056% w/v (10 Pa) hydrogels (Fig. 2A). After an additional 12 h, we observed a slight increase in viscoelasticity of all hydrogels (0.22% w/v to 780 Pa, 0.11% w/v to 84 Pa, and 0.056% w/v to 13 Pa) (Fig. 2B). The elastic modulus (G') data can be found in Supplementary Fig. S1. The 24-h gelation period is sufficient to completely crosslink all available thiol groups on the hydrogels at this HA:gelatin and PEGDA crosslinker composition[21]; indeed, further gelation time did not significantly increase substrate viscoelasticity (data not shown).

Defining HA hydrogel viscoelasticity, ultrastructure, and VEGF administration that support in vitro *tube morphogenesis*

The physical properties of hydrogels are determined by their composition and 3D ultrastructure (namely pore size, distribution, and connectivity), which are coupled with their viscoelasticity properties.[34] Specifically, in the HA hydrogels used for this study, the variation in PEGDA crosslinker concentrations might have affected not only their viscoelasticity but also their interior morphology, thereby altering cellular responses. Cord-blood-derived ECFCs were demonstrated to form functional and stable blood vessels *in vivo* compared to adult peripheral blood EPCs, which formed blood vessels that were unstable and that regressed rapidly.[8,35,36] We previously utilized ECFCs to study 2D *in vitro* capillary tube formation induced by substrate nanotopography,[37] patterned surfaces,[23] and matrix viscoelasticity.[22] In the last mentioned study, high concentrations of VEGF (i.e., 50 ng/mL) were demonstrated to induce 2D tubulogenesis on HA hydrogels. Therefore, to study 3D vascular morphogenesis in a controllable *in vitro* system, we encapsulated ECFCs within these HA hydrogels and cultured them in media supplemented with 50 ng/mL (high) VEGF. We first examined the optimized viscoelasticity of HA hydrogels, which supports 3D morphogenesis of ECFCs, and then determined the ultrastructure of these HA hydrogels and the effect of the VEGF administration method.

Viscoelasticity. We studied vascular morphogenesis by ECFCs in matrix with 0.22%, 0.11%, and 0.056% w/v PEGDA crosslinker, which correspond, respectively, to matrices with varying viscoelasticities—stiff, medium, and soft. We found that in the stiffest (0.22%) matrix, ECFCs remained rounded after 12 h and could not form CLS even after 96 h (Supplementary Fig. S2; Supplementary Data are available online at www.liebertonline.com/tea). Therefore, we focused on evaluating vascular morphogenesis in 0.11% and 0.056% substrates. After 24 h, sprouting was observed in both of these hydrogels (data not shown), and clear CLS formation occurred within 48 h (Fig. 3A). However, we observed that the structure of the CLSs formed in both of these hydrogels was dissimilar: when hydrogel viscoelasticity was reduced, we detected a significant increase in tube length (from 156 ± 6 μm on 0.11% matrix to 204 ± 27 μm on 0.056% matrix) and in tube area (from $471 \pm 73\,\mu m^2$ on 0.11% matrix to $856 \pm 133\,\mu m^2$ on 0.056% matrix) (Fig. 3Bii). Similarly, the

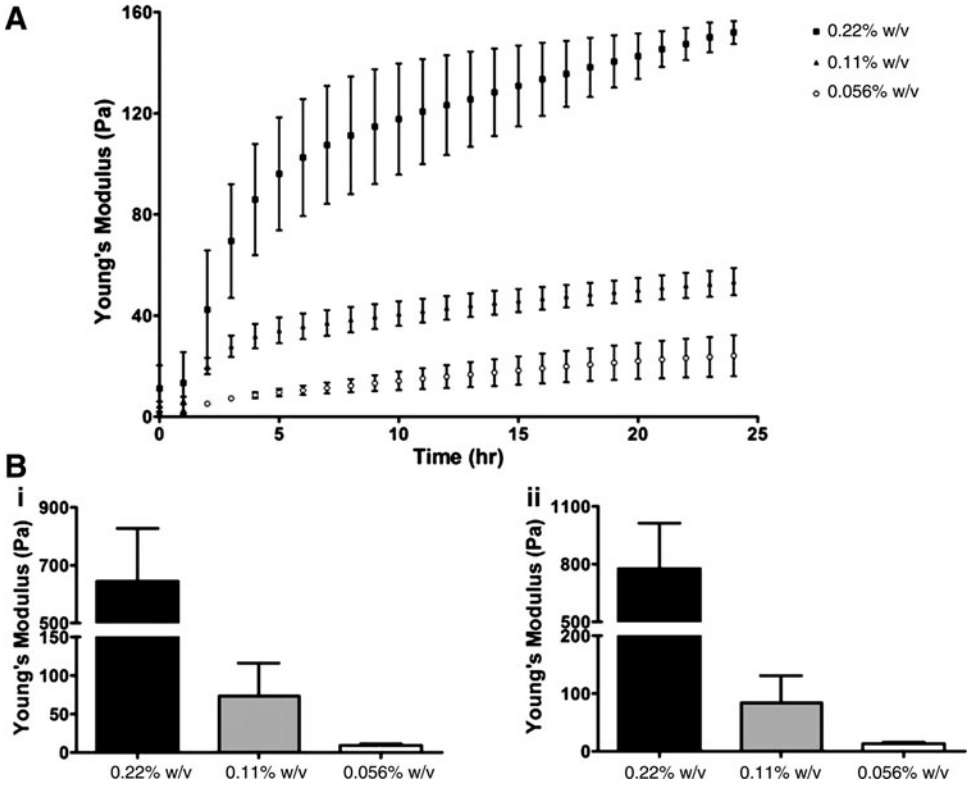

FIG. 2. Viscoelasticity of hydrogels. **(A)** Microrheology measurements of HA:gelatin in a 1:1 volume ratio with 0.22%, 0.11%, and 0.056% w/v of PEGDA crosslinker over 24 h of gelation show three distinct profiles of hydrogel mechanics. Values shown are means ± SD for Young's modulus (E) over 24 h during the *in situ* gelation (please see Supplementary Fig. S1 for elastic modulus [G'] data). **(B) (i)** After 12 h, the values of Young's modulus (viscoelasticity) were 640 ± 180 Pa for 0.22% w/v hydrogel, 73 ± 43 Pa for 0.11% w/v hydrogel, and 10 ± 2 Pa for 0.056% w/v hydrogel. **(ii)** After an additional 12-h gelation period, we observed a slight increase in viscoelasticity in all three hydrogels, with values of 780 ± 240, 84 ± 47, and 13 ± 3 Pa, respectively. HA, hyaluronic acid.

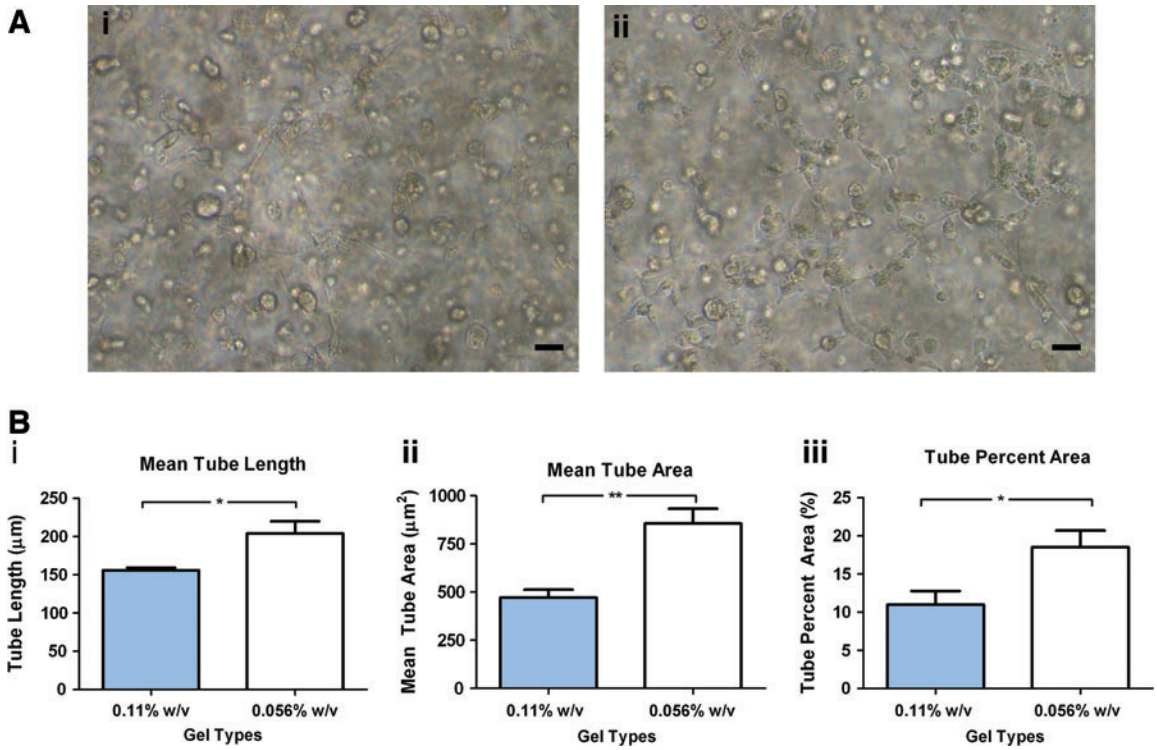

FIG. 3. Vascular tube morphogenesis by ECFCs. **(A)** Light microcopy images of CLSs formed in 0.11% (left) and 0.056% (right) after 48 h. **(B)** Analysis of CLSs using Metamorph software revealed that, as matrix viscoelasticity decreased, there were significant increases **(i)** of mean tube length, **(ii)** of mean tube area, and **(iii)** of the percent of area covered by CLSs. Significance levels were set at $*p < 0.05$ and $**p < 0.01$. Scale bar is 20 μm. CLS, capillary-like structure. Color images available online at www.liebertonline.com/tea

percentage of area covered by CLSs also increased—from 11% ± 3% on 0.11% matrix to 19% ± 4% on 0.056% matrix—with a decrease in hydrogel viscoelasticity (Fig. 3Biii). Fluorescence confocal microscope analyses show CLS forming in limited areas in 0.11% matrix, while distributed throughout the 0.056% matrix (Fig. 4A). Using high magnification 3D z-stack confocal analysis, we further show that these structures are more evolved in 0.056% compared with 0.11% matrix (Fig. 4B; Supplementary Movies S1 and S2). Analysis of low magnification confocal images (representative images are presented in Supplementary Fig. S3) revealed that the percentage of sprouting cells participated in forming CLS is increased from 5.8% in the 0.11% matrix to 20.4% in the 0.056% matrix (Fig. 4C).

Ultrastructure. To further evaluate the effect of matrix physical properties on vascular morphogenesis, we analyzed the interior morphology of hydrogels with distinct matrix viscoelasticities. SEM revealed large microchannels with an average diameter of 200 μm in the softest substrate (Fig. 5). These enlarged microchannel networks found in the softest (0.056%) hydrogel could not be detected in the stiffer 0.22% and 0.11% hydrogels (Supplementary Fig. S4). Our data suggest that ECFCs were able to form better CLSs in the softest substrate partially because of this loose structure of microchannel networks.

VEGF. We previously demonstrated that high concentrations of VEGF are required for 2D ECFC tubulogenesis on these HA hydrogels. Here, we sought to determine whether such concentrations are required for 3D CLSs of ECFC in the same hydrogel system. We cultured ECFC-HA constructs in media supplemented with either 1 ng/mL (low) or 50 ng/mL (high) VEGF. Indeed, when supplementing the culture media with high concentrations of VEGF, CLSs could be observed in 0.11% or 0.056% w/v HA hydrogels, unlike when the culture was supplemented with low levels of VEGF (data not shown). We then examined whether the local delivery of VEGF in the ECFC microenvironment improved ECFC CLS formation. We both co-encapsulated high concentrations of VEGF (50 ng/mL) with ECFCs within the 0.11% and 0.056% w/v HA hydrogels and also cultured HA hydrogel constructs in media supplemented with the same high levels of VEGF. No significant differences could be observed when VEGF was encapsulated in the 0.11% hydrogels or only supplementing the culture media (Fig. 6A), whereas VEGF encapsulated in the 0.056% hydrogels increased mean tube area compared to only supplementing the culture media with VEGF (Fig. 6B). To further explain these observations, we studied VEGF release profile from both hydrogels. Throughout the first 12 h, more VEGF was released from the 0.056% compared to the 0.11% w/v HA hydrogels. The difference became significant after 24 h where 55% of the encapsulated VEGF was released from the 0.11% w/v hydrogels, whereas 70% of the encapsulated VEGF was released from the 0.056% w/v hydrogel. This significant difference persisted after 48 h, where 60% of the encapsulated VEGF was released from the 0.11% w/v hydrogels compared to 80% released from the 0.056% w/v hydrogels (Fig. 6C).

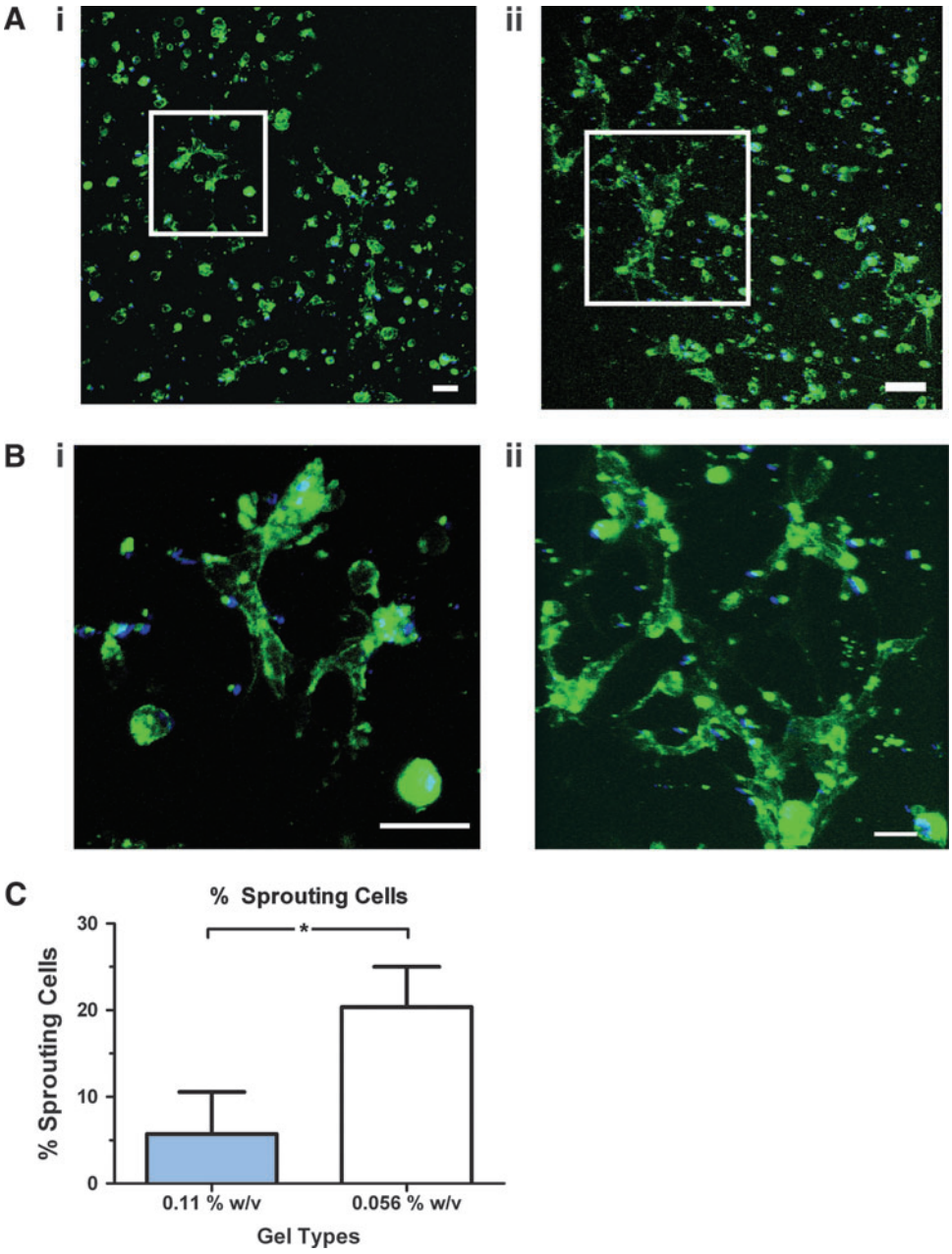

FIG. 4. Confocal images of CLSs by ECFCs. **(A)** Representative confocal images of nuclei (blue) and lectin (green) show distinctive CLS phenotype in **(i)** 0.11% and **(ii)** 0.056% w/v matrix. **(B)** High magnification image of the indicated white box show the complexity of the CLS formed in **(i)** 0.11% and **(ii)** 0.056% w/v matrix. Scale bars are 50 μm. **(C)** Quantification analysis of low magnification confocal images revealed that significantly more sprouting cells participated in CLS formation in 0.056% than in 0.11% w/v matrix.

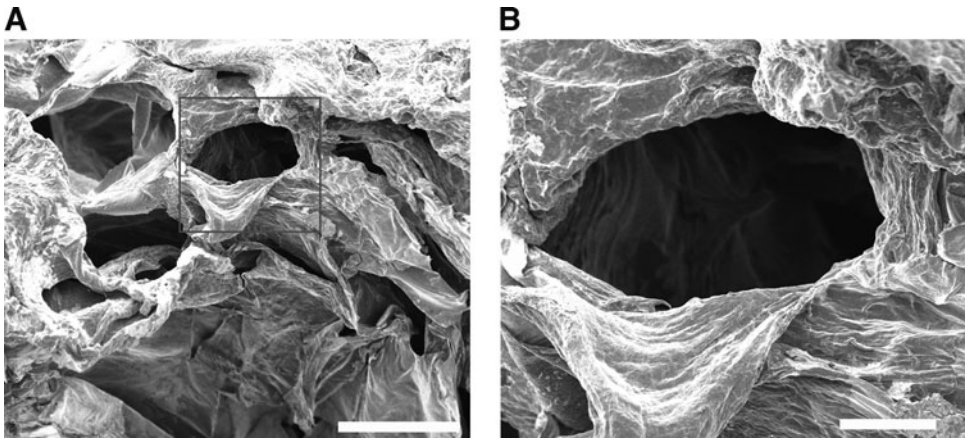

FIG. 5. Ultrastructure of HA hydrogels. **(A)** Scanning electron microscopy analysis revealed the interior morphology of a 0.056% matrix. Scale bar is 400 μm. **(B)** Higher magnification of the red box area indicated the average diameter of the microchannel. Scale bar is 100 μm.

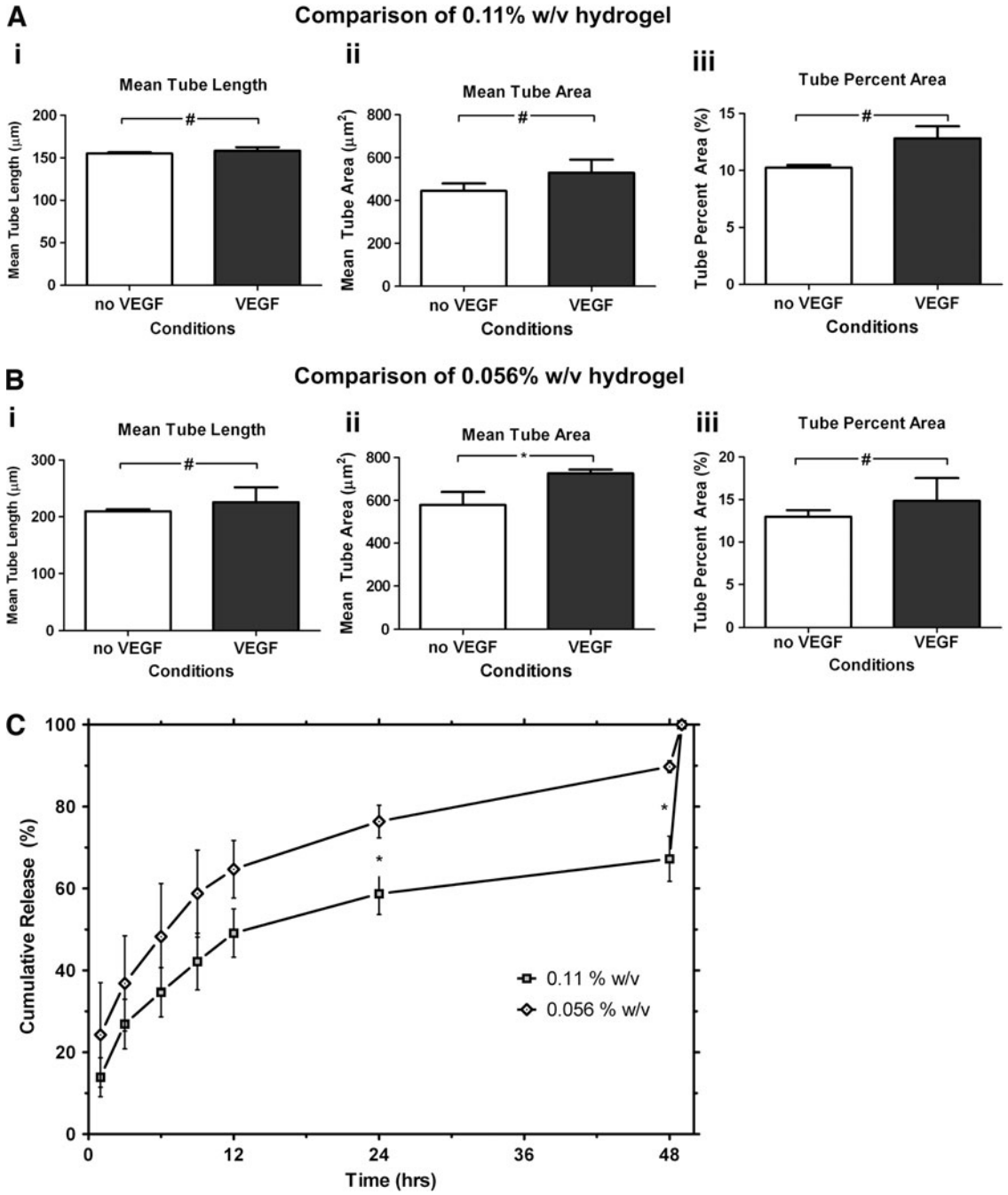

FIG. 6. The effect of encapsulating VEGF in the hydrogels. **(A)** Encapsulating VEGF in 0.11% w/v hydrogel does not significantly affect mean tube length **(i)**, mean tube area **(ii)**, or tube area percentage **(iii)**. **(B)** Encapsulating VEGF in 0.056% w/v hydrogel does not significantly affects mean tube length **(i)** and tube percent area **(iii)**, but significantly affects mean tube area **(ii)**. **(C)** VEGF release profile shows two distinct profiles for 0.11% and 0.056% w/v matrix. Significance levels were set at: $^{\#}p > 0.05$ and $^{*}p < 0.05$.

Discussion

Cellular therapy using EPCs for revascularization and to generate vascularized organ constructs to treat ischemia holds great promise for regenerative medicine. However, clinical trials involving direct injections of EPCs into the site of vascularization have resulted in inconsistent benefits, partly due to the limited survival of cells.[38,39] One approach to improving the efficiency and retention of cell delivery is to design biomaterials scaffolds that provide microenvironments that support vascular morphogenesis.[4,18,40] Generating a microvascular construct within a synthetic hydrogel that is xeno-free and tunable would provide a more clinically relevant alternative to enhance anastomosis in host

vasculatures.[41] Hydrogels that have properties like most soft tissues have been used to improve the delivery of EPCs and to restore blood flow in an ischemia model.[4,7]

In recent decades, the role of the natural ECM in vascular morphogenesis has been elucidated in great detail.[16,42] Collagen and fibrin gels have been used to study the effects of matrix viscoelasticity in vascular morphogenesis both *in vitro*[43] and *in vivo*.[36] However, due to the inherent limitations of these gels, it is important to notice that, in those studies, the influence of adhesion peptide density could not be easily differentiated from the effects of matrix viscoelasticity.[44] To address these issues, recent studies have utilized newly developed synthetic biomaterials to explore the effects of scaffold properties on the fate of stem cells[45–48] and on vascular morphogenesis.[18,49] In a previous study, we utilized HA hydrogels to investigate 2D vascular morphogenesis by ECFCs.[22] Using this controllable and well-defined system, we were able to decouple the effect of matrix viscoelasticity from changes in adhesive ligand density, which may alone affect vascular morphogenesis.[50] Here, utilizing HA hydrogels, we extended our previous study (a) to explore the 3D formation of CLSs over a range of elasticity that included materials softer than are currently available using *in vitro* angiogenesis models, including collagen and fibrin gels, and yet relevant for vascular morphogenesis (640 to 10 Pa) and (b) to determine how the physical properties of hydrogel and the method of administering VEGF affects CLS formation.

Determining if HA hydrogels are biologically relevant materials for angiogenesis is essential. We therefore first demonstrated that ECFCs can interact with these hydrogels through the HA receptors CD44 and CD168. We also found that these ECFCs expressed increased levels of hyaluronidase when cultured in media containing high levels of VEGF. In response to VEGF stimulation, ECFCs expressed levels of hyaluronidase comparable to colon cancer cells that are known to produce hyaluronidase during tumor growth and invasion.[31] Hyaluronidase production induced by VEGF may enable ECFCs to remodel HA hydrogels, to reduce the mechanical resistance of the ECM, and to migrate and reorganize into CLSs within HA hydrogels. However, 3D CLS formation was found to depend on the viscoelasticity and ultrastructure of the HA hydrogels. ECFCs remained rounded and could not form CLSs in the stiffest matrix, partly due to its small pore size and the complexity of its ultrastructure. We found that CLS formed best in the softest matrix, which has large microchannels and a loose ultrastructure. Altogether, our data suggest that the physical properties of HA hydrogel affect CLS formation.

Different studies have suggested that local delivery of growth factors in the cellular microenvironment better trigger desired cellular responses.[51,52] In our culture system, encapsulation of VEGF only slightly improves CLS formation in gels with soft viscoelasticity, but not CLSs formed within the medium gels. The release profile of VEGF indicates that after 24 h, more than half of the encapsulated VEGF is released from the hydrogels into the culture medium and that soft hydrogels exhibit faster release profile than the stiffer hydrogels, most likely due to looser interior ultrastructure. To some limited extent, the local delivery of VEGF enhances CLS formation in the soft hydrogels. Collectively, these data suggest that the local delivery of VEGF within the vascular cell microenvironment may affect cellular responses, but this depends on the properties of the synthetic environment (i.e., pore size, distribution, and connectivity). Softer matrix with looser interior network ultrastructure releases encapsulated VEGF rapidly, which may benefit the formation of vascularized construct *in vitro*. On the other hand, a stiffer matrix with more complex interior network ultrastructure retains encapsulated VEGF for a longer period of time, which may be beneficial for therapeutic angiogenesis *in vivo*. In the context of *in vitro* vascularization of engineered constructs for *in vivo* implantation, these results may suggest that an ideal scaffold should have a rapid VEGF release profile at the beginning of the culture period, followed by a sustained release of VEGF and other necessary GFs, to promote *in vivo* survival and integration. Please note that we did not test intermediate concentrations of VEGF (e.g., 10 ng/mg and 25 ng/mL) here, because, in our previous study, medium concentrations of VEGF supported 2D CLS formation less effectively than high concentrations.[22] We therefore do not dismiss the possibility that encapsulating these lower VEGF levels may enhance CLS formation significantly better than just supplementing media with such concentrations.

Collectively, these reported results have significant implications for designing biomaterials scaffolds to generate vascularized tissue constructs. Biologically relevant synthetic hydrogels with controllable matrix viscoelasticity and ultrastructure, as well as the method used to administer VEGF must be considered when engineering robust vascular constructs. Other parameters, such as the control over adhesive ligand density in the matrix and the use of perivascular cells, may need to be considered to form stable and functional vascular networks *in vivo*.[7,53,54]

Acknowledgments

We thank Dr. Merv C. Yoder from the Indiana University School of Medicine for providing ECFCs, Dr. Jennifer H. Elisseeff and Jeannine Coburn from The Johns Hopkins University (JHU) for assisting with microrheology measurements, Michael McCaffery from the Integrated Imaging Center at JHU for SEM processing and imaging, and Sravanti Kusuma for helping with flow cytometry analysis. This research was partially funded by an AHA Scientist Development Grant and a March of Dimes-O'Conner Starter Scholar Award (both for S.G), and by NIH grant U54CA143868.

Disclosure Statement

No competing financial interests exist.

References

1. Asahara, T., Murohara, T., Sullivan, A., Silver, M., van der Zee, R., Li, T., *et al.* Isolation of putative progenitor endothelial cells for angiogenesis. Science **275,** 964, 1997.
2. Hill, J.M., Zalos, G., Halcox, J.P., Schenke, W.H., Waclawiw, M.A., Quyyumi, A.A., *et al.* Circulating endothelial progenitor cells, vascular function, and cardiovascular risk. N Engl J Med **348,** 593, 2003.
3. Urbich, C., and Dimmeler, S. Endothelial progenitor cells: characterization and role in vascular biology. Circ Res **95,** 343, 2004.
4. Silva, E.A., Kim, E.-S., Kong, H.J., and Mooney, D.J. Material-based deployment enhances efficacy of endothelial progenitor cells. Proc Natl Acad Sci USA **105,** 14347, 2008.

5. Schatteman, G.C., Hanlon, H.D., Jiao, C., Dodds, S.G., and Christy, B.A. Blood-derived angioblasts accelerate blood-flow restoration in diabetic mice. J Clin Invest **106,** 571, 2000.
6. Shepherd, B.R., Enis, D.R., Wang, F., Suarez, Y., Pober, J.S., and Schechner, J.S. Vascularization and engraftment of a human skin substitute using circulating progenitor cell-derived endothelial cells. FASEB J **20,** 1739, 2006.
7. Melero-Martin, J.M., De Obaldia, M.E., Kang, S.Y., Khan, Z.A., Yuan, L., Oettgen, P., *et al.* Engineering robust and functional vascular networks *in vivo* with human adult and cord blood-derived progenitor cells. Circ Res **103,** 194, 2008.
8. Au, P., Daheron, L.M., Duda, D.G., Cohen, K.S., Tyrrell, J.A., Lanning, R.M., *et al.* Differential *in vivo* potential of endothelial progenitor cells from human umbilical cord blood and adult peripheral blood to form functional long-lasting vessels. Blood **111,** 1302, 2008.
9. Hirschi, K.K., Ingram, D.A., and Yoder, M.C. Assessing identity, phenotype, and fate of endothelial progenitor cells. Arterioscler Thromb Vasc Biol **28,** 1584, 2008.
10. Ingram, D.A., Mead, L.E., Moore, D.B., Woodard, W., Fenoglio, A., and Yoder, M.C. Vessel wall-derived endothelial cells rapidly proliferate because they contain a complete hierarchy of endothelial progenitor cells. Blood **105,** 2783, 2005.
11. Yoder, M.C. Is endothelium the origin of endothelial progenitor cells? Arterioscler Thromb Vasc Biol **30,** 1094, 2010.
12. Asahara, T., Takahashi, T., Masuda, H., Kalka, C., Chen, D., Iwaguro, H., *et al.* VEGF contributes to postnatal neovascularization by mobilizing bone marrow-derived endothelial progenitor cells. EMBO J **18,** 3964, 1999.
13. Li, B., Sharpe, E.E., Maupin, A.B., Teleron, A.A., Pyle, A.L., Carmeliet, P., *et al.* VEGF and PlGF promote adult vasculogenesis by enhancing EPC recruitment and vessel formation at the site of tumor neovascularization. FASEB J **20,** 1495, 2006.
14. Toole, B.P. Hyaluronan in morphogenesis. Semin Cell Dev Biol **12,** 79, 2001.
15. Toole, B.P. Hyaluronan: from extracellular glue to pericellular cue. Nat Rev Cancer **4,** 528, 2004.
16. Davis, G.E., Kon, W., and Stratman, A.N. Mechanisms controlling human endothelial lumen formation and tube assembly in three-dimensional extracellular matrices. Birth Defects Res C Embryo Today **81,** 270, 2007.
17. Kniazeva, E., and Putnam, A.J. Endothelial cell traction and ECM density influence both capillary morphogenesis and maintenance in 3-D. Am J Physiol Cell Physiol **297,** C179, 2009.
18. Moon, J.J., Saik, J.E., Poche, R.A., Leslie-Barbick, J.E., Lee, S.H., Smith, A.A., *et al.* Biomimetic hydrogels with pro-angiogenic properties. Biomaterials **31,** 3840, 2010.
19. Sieminski, A.L., Hebbel, R.P., and Gooch, K.J. The relative magnitudes of endothelial force generation and matrix stiffness modulate capillary morphogenesis *in vitro*. Exp Cell Res **297,** 574, 2004.
20. Burdick, J.A., Chung, C., Jia, X., Randolph, M.A., and Langer, R. Controlled degradation and mechanical behavior of photopolymerized hyaluronic acid networks. Biomacromolecules **6,** 386, 2005.
21. Vanderhooft, J.L., Alcoutlabi, M., Magda, J.J., and Prestwich, G.D. Rheological properties of cross-linked hyaluronan-gelatin hydrogels for tissue engineering. Macromol Biosci **9,** 20, 2009.-
22. Hanjaya-Putra, D., Yee, J., Ceci, D., Truitt, R., Yee, D., and Gerecht, S. Vascular endothelial growth factor and substrate mechanics regulate *in vitro* tubulogenesis of endothelial progenitor cells. J Cell Mol Med **14,** 2436, 2010.
23. Dickinson, L.E., Moura, M.E., and Gerecht, S. Guiding endothelial progenitor cell tube formation by pattered fibronectin surfaces. Soft Matter **6,** 5109, 2010.
24. Mammoto, A., Connor, K.M., Mammoto, T., Yung, C.W., Huh, D., Aderman, C.M., *et al.* A mechanosensitive transcriptional mechanism that controls angiogenesis. Nature **457,** 1103, 2009.
25. Boudou, T., Ohayon, J., Picart, C., and Tracqui, P. An extended relationship for the characterization of Young's modulus and Poisson's ratio of tunable polyacrylamide gels. Biorheology **43,** 721, 2006.
26. Sun, G.M., and Chu, C.C. Synthesis, characterization of biodegradable dextran-allyl isocyanate-ethylamine/polyethylene glycol-diacrylate hydrogels and their *in vitro* release of albumin. Carbohydr Polym **5,** 273, 2006.
27. Sun, G., Shen, Y.-I., Ho, C.C., Kusuma, S., and Gerecht, S. Functional groups affect physical and biological properties of dextran-based hydrogels. J Biomed Mater Res A **93,** 1080, 2010.
28. Sun, G., Shen, Y.-I., Kusuma, S., Fox-Talbot, K., Steenbergen, C.J., and Gerecht, S. Functional neovascularization of biodegradable dextran hydrogels with multiple angiogenic growth factors. Biomaterials **32,** 95, 2011.
29. Ausprunk, D.H. Distribution of hyaluronic acid and sulfated glycosaminoglycans during blood-vessel development in the chick chorioallantoic membrane. Am J Anat **177,** 313, 1986.
30. Yang, B., Hall, C.L., Yang, B.L., Savani, R.C., and Turley, E.A. Identification of a novel heparin binding domain in RHAMM and evidence that it modifies HA mediated locomotion of*ras*-transformed cells. J Cell Biochem **56,** 455, 1994.
31. Sugahara, K.N., Hirata, T., Hayasaka, H., Stern, R., Murai, T., and Miyasaka, M. Tumor cells enhance their own CD44 cleavage and motility by generating hyaluronan fragments. J Biol Chem **281,** 5861, 2006.
32. Shu, X.Z., Ahmad, S., Liu, Y., and Prestwich, G.D. Synthesis and evaluation of injectable, *in situ* crosslinkable synthetic extracellular matrices for tissue engineering. J Biomed Mater Res A **79,** 902, 2006.
33. Gerecht, S., Burdick, J.A., Ferreira, L.S., Townsend, S.A., Langer, R., and Vunjak-Novakovic, G. Hyaluronic acid hydrogel for controlled self-renewal and differentiation of human embryonic stem cells. Proc Natl Acad Sci USA **104,** 11298, 2007.
34. Sun, G., Shen, Y.I., Ho, C.C., Kusuma, S., and Gerecht, S. Functional groups affect physical and biological properties of dextran-based hydrogels. J Biomed Mater Res A **93,** 1080, 2010.
35. Ingram, D.A., Mead, L.E., Tanaka, H., Meade, V., Fenoglio, A., Mortell, K., *et al.* Identification of a novel hierarchy of endothelial progenitor cells using human peripheral and umbilical cord blood. Blood **104,** 2752, 2004.
36. Critser, P.J., Kreger, S.T., Voytik-Harbin, S.L., and Yoder, M.C. Collagen matrix physical properties modulate endothelial colony forming cell-derived vessels *in vivo*. Microvasc Res **80,** 23, 2010.
37. Bettinger, C.J., Zhang, Z., Gerecht, S., Borenstein, J., and Langer, R. Enhancement of *in vitro* capillary tube formation by substrate nanotopography. Adv Mater **20,** 99, 2008.
38. Assmus, B., Honold, J., Schächinger, V., Britten, M.B., Fischer-Rasokat, U., Lehmann, R., *et al.* Transcoronary transplantation of progenitor cells after myocardial infarction. N Engl J Med **355,** 1222, 2006.

39. March, K.L., and Johnstone, B.H. Cellular approaches to tissue repair in cardiovascular disease: the more we know, the more there is to learn. Am J Physiol Heart Circ Physiol **287,** H458, 2004.
40. Hanjaya-Putra, D., and Gerecht, S. Vascular engineering using human embryonic stem cells. Biotechnol Prog **25,** 2, 2009.
41. Hanjaya-Putra, D., and Gerecht, S. Preview. Mending the failing heart with a vascularized cardiac patch. Cell Stem Cell **5,** 575, 2009.
42. Stratman, A.N., Malotte, K.M., Mahan, R.D., Davis, M.J., and Davis, G.E. Pericyte recruitment during vasculogenic tube assembly stimulates endothelial basement membrane matrix formation. Blood **114,** 5091, 2009.
43. Deroanne, C.F., Lapiere, C.M., and Nusgens, B.V. *In vitro* tubulogenesis of endothelial cells by relaxation of the coupling extracellular matrix-cytoskeleton. Cardiovasc Res **49,** 647, 2001.
44. Guilak, F., Cohen, D.M., Estes, B.T., Gimble, J.M., Liedtke, W., and Chen, C.S. Control of stem cell fate by physical interactions with the extracellular matrix. Cell Stem Cell **5,** 17, 2009.
45. Khetan, S., Katz, J.S., and Burdick, J.A. Sequential crosslinking to control cellular spreading in 3-dimensional hydrogels. Soft Matter **5,** 1601, 2009.
46. Huebsch, N., Arany, P.R., Mao, A.S., Shvartsman, D., Ali, O.A., Bencherif, S.A., *et al.* Harnessing traction-mediated manipulation of the cell/matrix interface to control stem-cell fate. Nat Mater **9,** 518, 2010.
47. Engler, A.J., Sen, S., Sweeney, H.L., and Discher, D.E. Matrix elasticity directs stem cell lineage specification. Cell **126,** 677, 2006.
48. Khetan, S., and Burdick, J.A. Patterning network structure to spatially control cellular remodeling and stem cell fate within 3-dimensional hydrogels. Biomaterials **31,** 8228, 2010.
49. Sieminski, A.L., Was, A.S., Kim, G., Gong, H., and Kamm, R.D. The stiffness of three-dimensional ionic self-assembling peptide gels affects the extent of capillary-like network formation. Cell Biochem Biophys **49,** 73, 2007.
50. Ingber, D.E., and Folkman, J. Mechanochemical switching between growth and differentiation during fibroblast growth factor-stimulated angiogenesis *in vitro*: Role of extracellular matrix. J Cell Biol **109,** 317, 1989.
51. Ehrbar, M., Metters, A., Zammaretti, P., Hubbell, J.A., and Zisch, A.H. Endothelial cell proliferation and progenitor maturation by fibrin-bound VEGF variants with differential susceptibilities to local cellular activity. J Control Release **101,** 93, 2005.
52. Ehrbar, M., Djonov, V.G., Schnell, C., Tschanz, S.A., Martiny-Baron, G., Schenk, U., *et al.* Cell-demanded liberation of VEGF121 from fibrin implants induces local and controlled blood vessel growth. Circ Res **94,** 1124, 2004.
53. Vo, E., Hanjaya-Putra, D., Zha, Y., Kusuma, S., and Gerecht, S. Smooth-muscle-like cells derived from human embryonic stem cells support and augment cord-like structures in vitro. Stem Cell Rev **6,** 237, 2010.
54. Au, P., Tam, J., Fukumura, D., and Jain, R.K. Bone marrow derived mesenchymal stem cells facilitate engineering of long-lasting functional vasculature. Blood **111,** 4551, 2008.

Address correspondence to:
Sharon Gerecht, Ph.D.
Department of Chemical and Biomolecular Engineering
The Johns Hopkins University
3400 N. Charles St.
Baltimore, MD 21218

E-mail: gerecht@jhu.edu.

Received: August 15, 2010
Accepted: January 18, 2011
Online Publication Date: February 28, 2011